SMA and CARMA observations of young brown dwarfs in ρ Ophiuchi and Taurus

P.-B. Ngoc[1,2,a], C.-F. Lee[2] and P. Ho[2,3]

[1] *Department of Physics, HCMIU, Vietnam National University Administrative Building, Block 6, Linh Trung Ward, Thu Duc District, HCM, Vietnam*
[2] *Institute of Astronomy and Astrophysics, Academia Sinica, PO Box 23-141, Taipei 106, Taiwan*
[3] *Harvard-Smithsonian Center for Astrophysics, Cambridge, MA 02138, USA*

Abstract. Molecular outflows provide vital information about the earliest stages in the birth of stars, studying the molecular outflow properties is therefore crucial for understanding how stars form. Brown dwarfs with masses between that of stars and planets are not massive enough to maintain stable hydrogen-burning fusion reactions during most of their lifetime. Their origins are subject to much debate in recent literature because their masses are far below the typical mass where core collapse is expected to occur. Based on Submillimeter Array (SMA) and Combined Array for Research in Millimeter-wave Astronomy (CARMA) observations, we present the first detections of bipolar molecular outflows from young brown dwarfs in ρ Ophiuchi and Taurus. Our results demonstrate that the bipolar molecular outflow operates down to brown dwarf masses, occurring in brown dwarfs as a scaled-down version of the universal process seen in young low-mass stars. This demonstrates that brown dwarfs and low-mass stars likely share the same formation mechanism.

1. INTRODUCTION

Star formation starts with collapse, accretion and launching of material into the bipolar outflow. It is thought that brown dwarfs could undergo the same stages of formation as stars and that they have a common origin [11]. However the typical masses of brown dwarfs, 15–75 M_J, are far below the typical Jeans mass in molecular clouds, and hence it is difficult to make a large number of them by direct gravitational collapse. Several brown dwarf formation mechanisms have been proposed [24], and more observations are needed to improve our understanding of the role of each of them. Observational evidences for accretion disks and jets from a few young brown dwarfs have been reported [4, 22]. The first detection of molecular outflows from a young brown dwarf in ρ Ophiuchi (ISO-Oph 102, 60 M_J) has been reported [18]. Our carbon monoxide (CO $J = 2 - 1$) map revealed a small-scale bipolar outflow with a size of about 500–1000 AU, an outflow mass of 10^{-4} $M_\odot$, and a mass loss rate of 10^{-9} $M_\odot\,\mathrm{yr}^{-1}$. These values are over 100 times smaller than that in low-mass stars. There are two important results from our detection. First, the detection demonstrates that brown dwarf formation undergoes a molecular outflow phase that is typical of young low-mass stars. This therefore supports the scenario that brown dwarfs do form like low-mass stars, e.g., by the turbulent fragmentation process, which produces cores with a wide range of masses from brown dwarfs to low-mass stars [17]. Second, it provides morphological properties of the molecular outflows to constrain the formation mechanism of outflows in the substellar domain. In short, there are currently two standard models: (1) The jet-driven

[a]e-mail: `pbngoc@hcmiu.edu.vn`

Table 1. Young Brown Dwarfs in ρ Ophiuchi and Taurus observed with SMA and CARMA.

Target	Mass (M_J)	Region	$\log(\dot{M})$ ($M_\odot\,\mathrm{yr}^{-1}$)	FELs	Array	References[a]
ISO-Oph 32	40	ρ Oph	−9.8	Yes (weak)	SMA	[16]
ISO-Oph 102	60	ρ Oph	−8.9	Yes (strong)	SMA	[16]
2M 0441	35	Taurus	−11.3	—	CARMA	[15]
2M 0439	50	Taurus	−11.3	—	CARMA	[15]
MHO 5	90	Taurus	−10.8	Yes (strong)	SMA	[14]

[a] References for mass estimate, accretion rate, and forbidden emission line (FEL) detection.

bow-shock model [12, 19] proposed that a jet propagates into the ambient material and forms a bow-shock surface at the head of the jet. As the bow shock moves away from the young star, it interacts with the ambient material and produces molecular outflows in a bow-shock position-velocity (PV) structure. (2) The wind-driven-shell model [21] proposed that the young star expels a wide-angle magnetized wind that radially sweeps up the ambient material, producing molecular outflows in a parabolic PV structure. In the low-mass domain, some observations have been made to test those models [8]. In the substellar domain, the first bow-shock PV structure has been observed in the brown dwarf ISO-Oph 102 [18], supporting the jet-driven bow-shock model.

Here we report our SMA and CARMA observations of 4 brown dwarfs and 1 very low-mass star in two star-forming regions ρ Ophiuchi and Taurus.

2. SAMPLE SELECTION

We have selected 5 targets in ρ Ophiuchi and Taurus (see Table 1) with masses ranging from 30 to 90 M_J, one of them (MHO 5) is a very low-mass star. All these objects are strong accretors [14–16]. Three of them (ISO-Oph 102, MHO 5, ISO-Oph 32) show forbidden emission lines (FELs) that could be associated with outflow activities, they are therefore good targets for our molecular outflow search. The Hα accretion emission profile of ISO-Oph 102 particularly shows an extreme P Cygni profile [16] with a dip on the blueward side, indicating a mass loss process analogous to that seen in higher mass T Tauri stars. In addition, the detection of the blue-shifted jet component of ISO-Oph 102 has been reported [22].

3. OBSERVATIONS AND DATA REDUCTION

3.1 SMA

We have observed the two brown dwarfs ISO-Oph 102 and ISO-Oph 32 and the very low-mass star (MHO5) with the receiver band at 230 GHz of the SMA[1] [5]. Both 2 GHz-wide sidebands, which are separated by 10 GHz, were used. The SMA correlator was configured with high spectral resolution bands of 512 channels per chunk of 104 MHz for ^{12}CO, ^{13}CO, and C^{18}O $J = 2 \rightarrow 1$ lines, giving a channel spacing of 0.27 km s^{-1}. A lower resolution of 3.25 MHz per channel was set up for the remainder of each sideband. Strong quasars have been observed for gain (e.g., $1625 - 254$, $0428 + 329$) and passband (e.g., 3C 279, 3C 454.3) calibration. Uranus was used for flux calibration. The data were calibrated using the MIR software package and further analysis was carried out with the MIRIAD package adapted for the SMA. The compact configuration was used, resulting a synthesized beam of about $3''.6 \times 2''.8$.

---

[1] The Submillimeter Array is a joint project between the Smithsonian Astrophysical Observatory and the Academia Sinica Institute of Astronomy and Astrophysics and is funded by the Smithsonian Institution and the Academia Sinica.

The rms sensitivity was about 1 mJy for the continuum, using both sidebands and $\sim 0.2\,\mathrm{Jy\,beam^{-1}}$ per channel for the line data. The primary FWHM beam is about $50''$ at the observed frequencies.

3.2 CARMA

The two least massive brown dwarfs 2M 0439 and 2M 0441 in our sample were observed with CARMA in the D configuration (a beam size of $2.4'' \times 2.0''$) at 230 GHz. All three 500 MHz-wide bands (1.5 GHz maximum bandwidth per sideband), which may be positioned independently with the IF bandwith, were used for CO search with different spectral resolutions. These bands were configured with channel widths of 0.122 MHz or $0.16\,\mathrm{km\,s^{-1}}$, 0.488 MHz or $0.64\,\mathrm{km\,s^{-1}}$, and 31.25 MHz or $40.7\,\mathrm{km\,s^{-1}}$. The quasars 3C 111 and 3C 84 have been observed for gain passband, and flux calibration. The data were calibrated using the MIRIAD package optimized for the CARMA. The synthesized beam sizes are about $2''.6 \times 2''.5$ and $2''.0 \times 1''.9$ for 2M 0439 and 2M 0441, respectively. The primary FWHM beam is about $36''$ at 230 GHz.

4. RESULTS AND DISCUSSION

4.1 ρ Ophiuchi: ISO-Oph 102 and ISO-Oph 32

4.1.1 ISO-Oph 102

The detection of the bipolar molecular outflow from ISO-Oph 102 has been reported [18]. Figure 1 shows an overlay of a near-infrared image and the integrated intensity in the carbon monoxide (CO $J = 2 - 1$) line emission from the brown dwarf. Two spatially resolved blue- and red-shifted CO components are symmetrically displaced on opposite sides of the brown dwarf position, with the size of each lobe of about $8''$ corresponding to 1000 AU in length. This is similar to the typical pattern of bipolar molecular outflows as seen in young stars [7]. We estimated the outflow properties using the standard method [1, 3]. The outflow mass and the mass-loss rate are $1.6 \times 10^{-4}\,M_\odot$ and $1.4 \times 10^{-9}\,M_\odot\,\mathrm{yr}^{-1}$, respectively. These values are over 2 orders of magnitude smaller than the typical ones for T Tauri stars, demonstrating that the molecular outflow in brown dwarfs is a scaled-down version of that in low-mass stars. One should note that the mass-loss rate from ISO-Oph 102 is approximately equal to its accretion rate of $1.3 \times 10^{-9}\,M_\odot\,\mathrm{yr}^{-1}$ [16]. From our millimeter continuum data and our analysis of Spitzer infrared photometry, we estimated that the brown dwarf has a disk with a mass of $8 \times 10^{-3}\,M_\odot$, an inclination angle between $63°$ and $66°$, an outer disk radius of 80 AU. This immediately explains the non-detection of the red-shifted optical jet component, estimated to be about 15 AU in length as reported in the previous observation [22]. Since the projected disk radius is larger than the jet length, the disk therefore hides the red-shifted jet component from our view.

The two outflow components with a wide range of velocity (see Figure 2) show a bow shock structure, an effect of the interaction between the jet propagation and the ambient material, which appears very similar to the bow shock phenomena as seen in young stars [8]. Such a CO outflow morphology suggests that the jet-driven bow shock model (e.g., [12]) may be at work in ISO-Oph 102.

We also examine the possibility that the emission might be due to bound motions and not outflow emission. This would require an interior mass [7] of $2.7 M_\odot$ for an outflow size of 1000 AU with a velocity of $2.2\,\mathrm{km\,s^{-1}}$ (the observed maximum flow velocity), which is significant larger than the core mass of $< 0.4\,M_\odot$ within the same radius [13, 25]. We therefore conclude that the detected emission is from the outflow.

It is worthy to note that the IRS infrared (7.5–14.3 μm) [6] spectra of ISO-Oph 102 shows crystalline silicate features: enstatite ($MgSiO_3$) at 9.3 μm and very strong forsterite (Mg_2SiO_4) at 11.3 μm [18]. This provides a direct evidence of grain growth and dust settling, indicating the object is in the transition phase between the class II and III (a class with an optically thin disk) and the brown dwarf is reaching
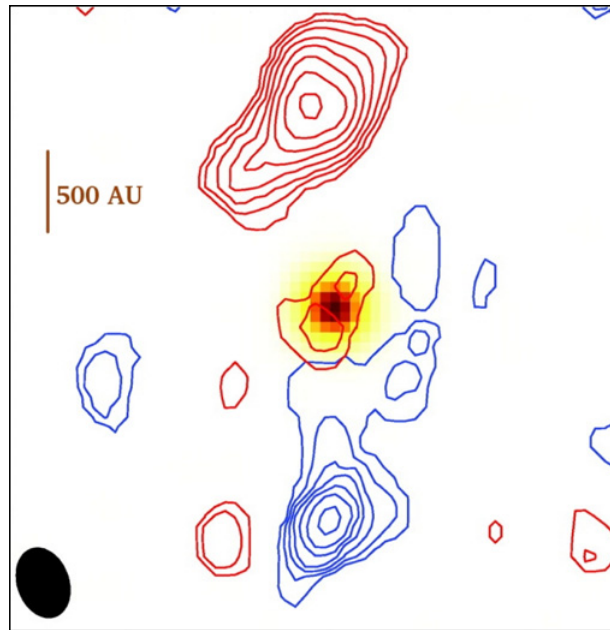
Figure 1. An overlay of the J-band (1.25 μm) near-infrared Two Micron All Sky Survey (2MASS) image of ISO-Oph 102 and the integrated intensity in the carbon monoxide (CO $J = 2 - 1$) line emission from 3.8 to 7.7 km s^{-1} line-of-sight velocities. The blue and red contours represent the blue-shifted (integrated over 3.8 and 5.9 km s^{-1}) and red-shifted (integrated over 5.9 and 7.7 km s^{-1}) emissions, respectively. The contours are $3, 6, 9, \ldots$ times the rms of 0.15 Jy beam^{-1} km s^{-1}. The brown dwarf is visible in the J-band image. The position angle of the outflow is about 3°. The peaks of the blue- and red-shifted components are symmetric to the center of the brown dwarf with an offset of 10″. The synthesized beam is shown in the bottom left corner.
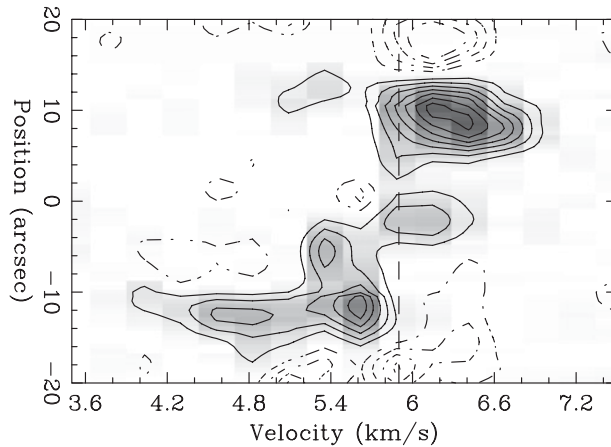
Figure 2. Position-Velocity (PV) cut diagram for CO $J = 2 \rightarrow 1$ emission from ISO-Oph 102 at a position angle of 3°. The contours are $-12, -9, -6, -3, 3, 6, 9, 12, \ldots$ times the rms of 0.2 Jy beam^{-1}. The systemic velocity of the brown dwarf, which is estimated by an average of the velocities of red- and blue-shifted components, is indicated by the dashed line. Our value of 5.9 ± 0.27 km s^{-1} is consistent with the previously measured value [22] of 7 ± 8 km s^{-1} within the error bar. Both blue- and red-shifted components shows a wide range of the velocity in their structure, which appears to be the bow-shock surfaces as observed in young stars [8]. These surfaces are formed at the head of the jet and accelerate the material in the bow-shock sideways (e.g., [12]).
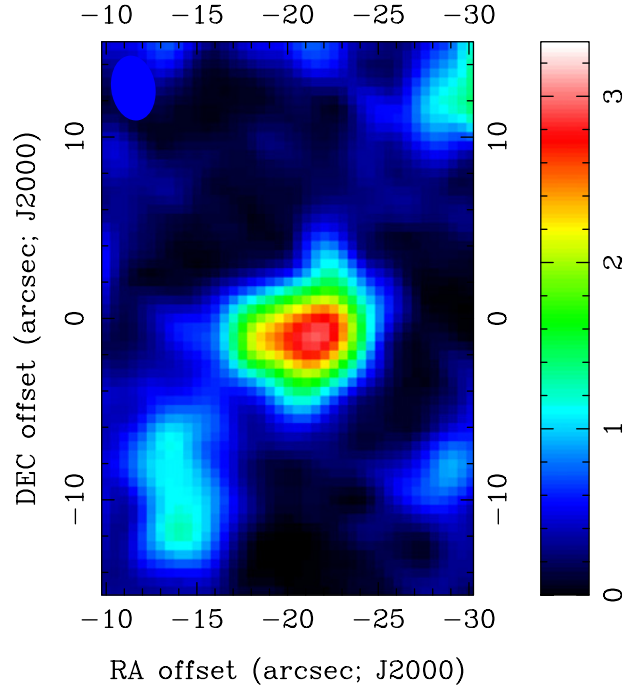
Figure 3. The integrated intensity in the carbon monoxide (CO $J = 2 - 1$) line emission from a proto-brown dwarf candidate over the line-of-sight velocity range from 3.5 to 6.4 km s^{-1}. The color bar indicates the intensity scale in Jy/beam. The synthesized beam is shown in the top left corner.

the final mass. Furthermore, since the outflow sweeps away the gas and dust in the vicinity of the young brown dwarf, the coexistence of molecular outflow and crystallization therefore favors the rocky planet formation around this young brown dwarf.

4.1.2 ISO-Oph 32

ISO-Oph 32 is an accretor [16]. A weak detection of its optical jet has recently reported [23] with a signal-to-noise ratio of just above 4. However, we did not detect any molecular outflow that would be expected to be entrained by the jet. The CO outflow emission from the source is likely too weak to be detectable with one SMA track. Deeper observations are needed to search for molecular outflows from the brown dwarf and to support Whelan et al.'s detection of the optical jet.

4.2 Taurus: MHO 5, 2M 0439, and 2M 0441

4.2.1 MHO 5

MHO 5 is a very low-mass star. We detect a bipolar molecular outflow from MHO 5. This is the first detection of molecular outflows from a very low-mass star in Taurus. The outflow properties of MHO 5 are similar to what we have observed in ISO-Oph 102. The outflows have small-scales with sizes of about 500 AU. The outflow mass and the mass-loss rate are $0.7 \times 10^{-4} M_{\odot}$ and $0.9 \times 10^{-9} M_{\odot}$ yr^{-1}, respectively. These values are also over 2 orders of magnitude smaller than the typical ones for T Tauri stars. Our detection indicates that the molecular outflow is a universal process, occuring in both low (Taurus) and high (ρ Ophiuchi) density star-forming regions. Since the estimated mass of MHO 5 is 90 M$_J$, which is just above the hydrogen-burning limit, therefore our result once again demonstrates that
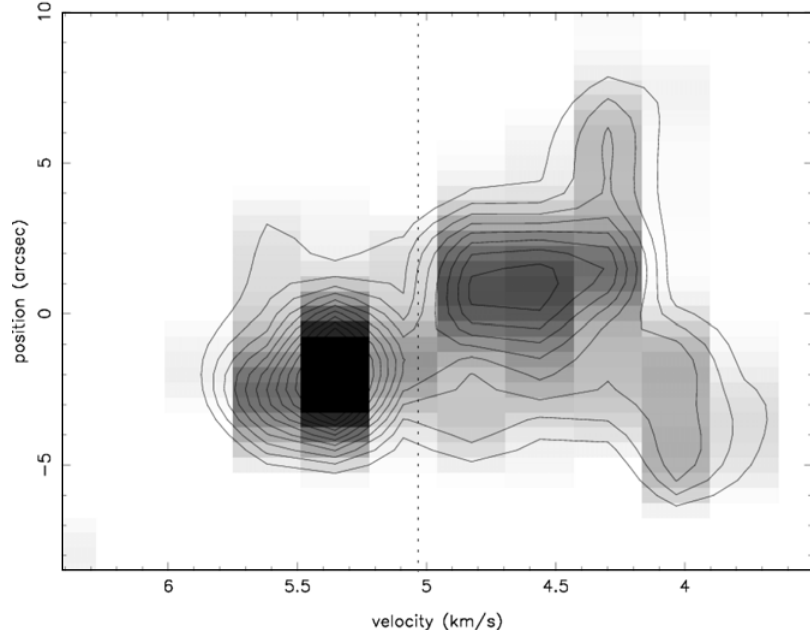
Figure 4. Position-Velocity (PV) cut diagram for CO $J = 2 \rightarrow 1$ emission from the proto-brown dwarf candidate at a position angle of $90°$. The contours are $3, 6, 9, 12, \ldots$ times the rms of $0.2\,\mathrm{Jy\,beam^{-1}}$. The systemic velocity of $\sim 5.0 \pm 0.27\,\mathrm{km\,s^{-1}}$ of the proto-brown dwarf candidate, which is estimated by an average of the velocities of red- and blue-shifted components, is indicated by the dashed line. Both blue- and red-shifted components show a small-scale and low-velocity flow similar to that observed in ISO-Oph 102.

objects at the bottom of the main sequence (very low-mass stars and brown dwarfs) likely share the same formation mechanism with low-mass stars.

4.2.2 2M 0439 and 2M 0441

No detection of forbidden emission lines in 2M 0439 (2M 04390396+2544264) and 2M 0441 (2M 04414825+2534304) has been reported so far. The dust continuum fluxes are $2.4 \pm 0.4\,\mathrm{mJy}$ and $2.2 \pm 0.4\,\mathrm{mJy}$ measured at the position of 2M 0439 and 2M 0441, respectively. Our measurements are consistent with the previous ones [20]. We did not detect any outflow emission from these two brown dwarfs. There are two possibilities to explain the non-detection of CO emission from these least massive brown dwarfs in our sample. First, their outflow emission might be too weak to be detectable. Second, since they are class II objects, therefore the outflow process might have stopped. One should note that the Hα accretion emission profile [15] of these sources has not shown any P Cygni profile, hence no evidence for outflow activities. This therefore likely supports the second possibility.

5. SUMMARY AND PERSPECTIVES

Here, we report the detections of the bipolar molecular outflows from the young brown dwarf ISO-Oph 102 (in ρ Ophiuchi) and the very low-mass star MHO 5 (in Taurus). First, our detections indicate that the bipolar molecular outflows in young brown dwarfs and very low-mass stars are very similar to that seen in young stars but scaled down by three and two orders of magnitude for the outflow mass and the mass-loss rate, respectively. Second, they demonstrate that the molecular outflow process in objects at the bottom of the main sequence occurs in both low and high density environments and support the

idea that they likely share the same formation mechanism with low-mass stars. This suggests that the terminal stellar/brown dwarf (even planetary) mass is not due to different formation mechanisms but more likely due to the initial mass of the cloud core.

As optical jets are not observable at very early phases of brown dwarf formation (e.g., class 0, brown dwarf cores), therefore only molecular outflows allow us to trace brown dwarf formation at these early phases. For example, Figure 3 shows the total intensity map of CO emission of a proto-brown dwarf candidate in ρ Ophiuchi. Its position-velocity diagram reveals the blue and red-shifted outflow components. The central object is only visible at millimeter wavelengths with a flux density of 8 ± 3 mJy (at 1.3 mm), suggesting that this object is in a very early phase of star formation. The small-scale and low-velocity outflow is similar to that observed in our brown dwarfs and to Bourke et al.'s observational result of a possible proto-brown dwarf [2], indicating that the source is likely a proto-brown dwarf. Further observations are requested to confirm its nature. The Atacama Large Millimeter/submillimeter Array (ALMA) with 10–100 times more sensitive and 10–100 times better angular resolution than the current mm/submm arrays is an excellent instrument for studying such these objects and searching proto-brown dwarfs/planetary mass objects at large-scales.

References

[1] P. André, J. Martín-Pintado, D. Despois, T. Montmerle, A&A, **236**, 180 (1990)

[2] T.L. Bourke, A. Crapsi, P.C. Myers, et al., ApJ, **633**, L129 (2005)

[3] S. Cabrit, C. Bertout, ApJ, **348**, 530 (1990)

[4] M. Fernández, F. Comerón, A&A, **380**, 264 (2001)

[5] P.T.P. Ho, J.M. Moran, K.Y. Lo, ApJ, **616**, L1 (2004)

[6] J.R. Houck, et al., ApJS, **154**, 18 (2004)

[7] C.J. Lada, ARA&A, **23**, 267 (1985)

[8] C.-F. Lee, L.G. Mundy, et al., ApJ, **542**, 925 (2000)

[9] R.M. Levreault, ApJ, **330**, 897 (1988a)

[10] R.M. Levreault, ApJS, **67**, 283 (1988b)

[11] K.L. Luhman, V. Joergens, C. Lada, J. Muzerolle, I. Pascucci, R. White, in *Protostars and Planets V*, edited by B. Reipurth, D. Jewitt, & K. Keil (Univ. Arizona Press, Tucson, 2007), p. 443

[12] C.R. Masson, L.M. Chernin, ApJ, **414**, 230 (1993)

[13] F. Motte, P. André, R. Neri, A&A, **336**, 150 (1998)

[14] J. Muzerolle, L. Hillendbrand, N. Calvet, C. Briceño, L. Hartmann, ApJ, **592**, 266 (2003)

[15] J. Muzerolle, K.L. Luhman, C. Briceño, L. Hartmann, N. Calvet, ApJ, **625**, 906 (2005)

[16] A. Natta, L. Testi, J. Muzerolle, S. Randich, F. Comerón, P. Persi, A&A, **424**, 603 (2004)

[17] P. Padoan, & A. Nordlund, ApJ, **617**, 559 (2004)

[18] N. Phan-Bao, et al., ApJ, **689**, L141 (2008)

[19] A. Raga, S. Cabrit, A&A, **278**, 267 (1993)

[20] A. Scholz, R. Jayawardhana, K. Wood, ApJ, **645**, 1498 (2006)

[21] F. Shu, et al., ApJ, **370**, L31 (1991)

[22] E.T. Whelan, et al., Nature, **435**, 652 (2005)

[23] E.T. Whelan, et al., ApJ, in press (arxiv:0910.2665), (2009)

[24] A. Whitworth, M.R. Bate, Å. Nordlund, B. Reipurth, H. Zinnecker, in *Protostars and Planets V*, edited by B. Reipurth, D. Jewitt, & K. Keil (Univ. Arizona Press, Tucson, 2007), p. 459

[25] K.E. Young, et al., ApJ, **644**, 326 (2006)